Inorg. Chem. **2004**, *43*, 2114–2124

Coordination Complexes of Molybdenum with 3,6-Di-*tert*-butylcatechol. Addition Products of DMSO, Pyridine *N*-oxide, and Triphenylarsine Oxide to the Putative [$Mo^{VI}O(3,6\text{-}DBCat)_2$] Monomer and Self-Assembly of the Chiral [$\{Mo^{VI}O(3,6\text{-}DBCat)_2\}_4$] Square

Cai-Ming Liu[†] and Ebbe Nordlander*

Inorganic Chemistry, Center for Chemistry and Chemical Engineering, Lund University, P.O. Box 124, Lund SE 221 00, Sweden

Derek Schmeh, Richard Shoemaker, and Cortlandt G. Pierpont*

Department of Chemistry and Biochemistry, University of Colorado, Boulder, Colorado 80309

Received December 11, 2003

Molybdenum complexes of 3,6-di-*tert*-butylcatechol have been prepared from the reaction between [$Mo(CO)_6$] and 3,6-di-*tert*-butyl-1,2-benzoquinone. A putative "[$MoO(3,6\text{-}DBCat)_2$]" monomer is assumed to form initially by reaction with trace quantities of oxygen. Condensation of the reaction mixture leads to the formation of oligomeric products, including the [$\{MoO(3,6\text{-}DBCat)_2\}_4$] chiral square isolated by chromatographic separation. Molybdenum centers at the corner of the square are bridged by oxo ligands centered along edges. Four-fold and inversion crystallographic symmetry gives tetramers as either ΛΛΛΛ or ΔΔΔΔ isomers, and the crystal structure consists of parallel columns of squares with the same chirality. Addition of O-Subst (O-Subst = dmso, pyridine *N*-oxide, triphenylarsine oxide) ligands to [$MoO(3,6\text{-}DBCat)_2$] occurs selectively to give *cis*-[$MoO(O\text{-}Subst)(3,6\text{-}DBCat)_2$] products. All three addition complexes are fluxional in solution. The temperature-dependent stereodymanic behavior of [$MoO(dmso)(3,6\text{-}DBCat)_2$] has been shown to occur via a trigonal prismatic intermediate (Bailar twist) that conserves the *cis* disposition of oxo and dmso ligands. Electrochemical and chemical reduction reactions have been investigated for [$MoO(dmso)(3,6\text{-}DBCat)_2$] with interest in displacement of SMe_2 with formation of *cis*-[$MoO_2(3,6\text{-}DBCat)_2]^{2-}$. Cyclic voltammetry shows an irreversible two-electron reduction for the complex at –0.852 V (vs Fc/Fc^+). Chemical reduction using $CoCp_2$ was observed to give a product with an electronic spectrum that is generally associated with *cis*-[$MoO_2(Cat)_2]^{2-}$ complexes. Structural characterization revealed that the product was [$CoCp_2$][$MoO(3,6\text{-}DBCat)_2$], possibly formed as the product of dmso displacement upon one-electron reduction of [$MoO(dmso)(3,6\text{-}DBCat)_2$].

Introduction

The coordination chemistry of molybdenum with ligands derived from *o*-benzoquinones has been of interest in studies on oxo coordination to complexes of Mo(VI).[1] Oxo and catecholate ligands both stabilize high oxidation state metal ions through strong σ and π donation to vacant metal orbitals, and both ligands are subject to displacement upon protonation (eq 1). Equilibria between coordinated oxo and catecholate

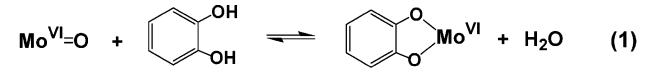

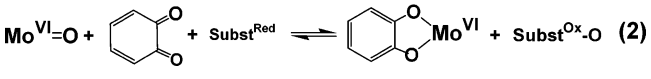

ligands are relevant to oxo transfer chemistry (eq 2) in processes that are influenced by coligand and catechol substituent effects, that may place the benzoquinone reduction potential on either side of the O_2 reduction potential (eq 3). The reaction between $Mo(CO)_6$ and 9,10-phenanthrenequinone (PhenBQ) was found to give the mixed catecholate/

* Authors to whom correspondence should be addressed. E-mail: Ebbe.Nordlander@inorg.lu.se (E.N.); Pierpont@Colorado.edu (C.G.P.).

[†] Present address: Organic Solids Laboratory, Center for Molecular Science, Institute of Chemistry, Chinese Academy of Sciences, Beijing 100080, China.

10.1021/ic0354264 CCC: $27.50
Published on Web 02/17/2004

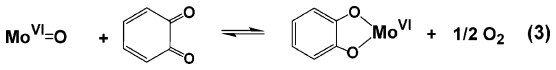

semiquinonate complex $[Mo^{V}(PhenCat)_2(PhenSQ)]$.[2] Hydrolysis under acidic conditions gave $[Mo^{VI}_2O_5(PhenSQ)_2]$.[3] The reaction between $[Mo(CO)_6]$ and 3,5-di-*tert*-butyl-1,2-benzoquinone (3,5-DBBQ) gave $[Mo^{VI}_2O_2(3,5\text{-}DBCat)_4]$, which could also be obtained by treating $[MoO_2(acac)_2]$ with H_2-3,5-DBCat.[4,5] These reactions illustrate the forward and reverse directions of reaction 1. The formation of $[Mo^{VI}_2O_2(3,5\text{-}DBCat)_4]$ from $[Mo(CO)_6]$ and 3,5-DBBQ was found to proceed by initial formation of $[Mo^{VI}(3,5\text{-}DBCat)_3]$ which reacted with trace quantities of dioxygen in the reaction medium (eq 3) to give the oxo product.[6] It was of interest to find that acidic hydrolysis of $[Mo^{VI}_2O_2(3,5\text{-}DBCat)_4]$ gave $[Mo^{VI}_2O_5(3,5\text{-}DBCat)_2]^{2-}$ rather than the more common *cis*-dioxomolybdenum(VI) species $[Mo^{VI}O_2(3,5\text{-}DBCat)_2]^{2-}$ that is known to form with a variety of other catecholate ligands.[7] In fact, we have been unable to observe the $[Mo^{VI}O_2(3,5\text{-}DBCat)_2]^{2-}$ dianion in any synthetic procedure, suggesting that the electron releasing property of the *tert*-butyl substituents of 3,5-DBCat destabilizes terminal oxo ligands coordinated to Mo(VI).

The coordination chemistry of molybdenum with the symmetrical 3,6-di-*tert*-butylcatecholate ligand has been described briefly, but none of the products of this chemistry have been characterized structurally.[8] Complexes formed with the 3,5-DBCat ligand are commonly dimeric or oligomeric with adjacent metal ions bridged by the oxygen atom at the 1-ring position. The 3,6-DBCat ligand appears unable to bridge metal ions due to the blocking effect of bulky substituents adjacent to both oxygen atoms.[9] Consequently, complexes of Mo(VI) formed with the 3,6-DBCat ligand should have different structural features and, potentially, different chemical properties from the products obtained with 3,5-DBCat. In this report we describe the structural, chemical, and electrochemical properties of the molybdenum complexes of 3,6-DBCat.[10] With the potential oxido lability of a transient $[Mo^{VI}O_2(3,6\text{-}DBCat)_2]^{2-}$ dianion, coupled oxo and electron transfer reactions will be of interest in the study of oxo coordination to the molybdenum complexes of 3,6-DBCat.

Experimental Section

Materials and Methods. 3,6-Di-*tert*-butyl-1,2-benzoquinone (3,6-DBBQ) was prepared by literature methods.[11] Other reagents and materials were purchased from commercial sources and were used as received. Reactions and solution studies were performed under nitrogen using deoxygenated solvents and standard Schlenk techniques. Solid-state infrared spectra were recorded on a Nicolet Avatar 360 FT-IR spectrometer with samples prepared as KBr disks. ^{1}H NMR spectra were recorded using Varian Unity 300 MHz and Inova(r) 500 MHz spectrometers. Fast atom bombardment (FAB) mass spectra were obtained on a JEOL SX-102 mass spectrometer using 3-nitrobenzyl alcohol as a matrix. UV−visible spectra were recorded on a Cary-Varian 2290 spectrophotometer, and cyclic voltammetric measurements were made inside a nitrogen filled glovebox using a PAR 263 potentiostat/galvanostat analyzer. Solutions of the complexes were dissolved in CH_2Cl_2 containing $(NBu_4)(PF_6)$ (ca. 0.1 M) as supporting electrolyte. Platinum wire working and counter electrodes were used with a $Ag/AgNO_3$ reference electrode. The Fc/Fc^+ couple appeared at +0.464 V (ΔE = 62 mV) vs SCE with this experimental arrangement, and the ferrocene couple was used as an internal reference.

[{MoO(3,6-DBCat)$_2$}$_4$]. 3,6-DBBQ (0.132 g, 0.6 mmol) and $[Mo(CO)_6]$ (0.079 g, 0.3 mmol) were refluxed in toluene (50 mL) under N_2 for 20 h. During this time the color of the solution turned from the green color of 3,6-DBBQ to deep blue-violet. The solution was reduced in volume, and the products were separated by TLC on silica plates using hexane/$CHCl_3$ (3:1) as eluent. At high R_f a deep blue product was obtained in 55% yield, which was subsequently identified as $[\{MoO(3,6\text{-}DBCat)_2\}_4]$. Other fractions obtained included unreacted 3,6-DBBQ and $[Mo(CO)_6]$, and a dark blue fraction that appeared to contain (from mass spectral analysis) $\{MoO(3,6\text{-}DBCat)_2\}_n$ oligomers and $[Mo(3,6\text{-}DBCat)_3]$.

$[\{MoO(3,6\text{-}DBCat)_2\}_4]$: ^{1}H NMR (300 MHz, C_6D_6, ppm) 6.493 (s, $2H_{ring}$), 1.290 (s, $9H_{Bu}$), 1.206 (s, $9H_{Bu}$); UV−vis ($CHCl_3$, λ_{max}(nm)) 278 ($\epsilon = 10.7 \times 10^3$ M^{-1} cm^{-1}), 320 (9.4×10^3 M^{-1} cm^{-1}), 620 (9.2×10^3 M^{-1} cm^{-1}); IR (KBr, cm^{-1}): 1729 (m), 1626 (m), 1581 (m), 1482 (m), 1462 (m), 1361 (w), 1339 (w), 1262 (vs), 1200 (m), 1096 (vs), 1024 (vs), 990 (m), 948 (w), 802 (vs), 757 (s); FAB$^+$-MS (*m*/*z*) 2210 $[\{MoO(3,6\text{-}DBCat)_2\}_4{}^+]$, 554 $[MoO(3,6\text{-}DBCat)_2{}^+]$.

***cis*-[Mo(O-^{i}Pr)$_2$(3,6-DBCat)$_2$].** A sample of $[\{MoO(3,6\text{-}DBCat)_2\}_4]$ (250 mg) was dissolved in hexane (25 mL), and *i*-propanol (~5 mL) was layered on top of the solution. As the *i*-propanol diffused through the solution, the color changed from the dark violet color of the tetramer to deep purple. The solution was reduced in volume under a flow of N_2, and dark purple crystals of $[Mo(O\text{-}^iPr)_2(3,6\text{-}DBCat)_2]$ formed in 75% yield.

(1) (a) Larson, M. L.; Moore, F. W. *Inorg. Chem.* **1966**, *5*, 801. (b) Cleland, W. E., Jr.; Barnhart, K. M.; Yamanouchi, K.; Collison, D.; Mabbs, F. E.; Ortega, R. B.; Enemark, J. H. *Inorg. Chem.* **1987**, *26*, 1017. (c) Chisholm, M. H.; Clark, D. L.; Errington, R. J.; Folting, K.; Huffman, J. C. *Inorg. Chem.* **1988**, *27*, 2059. (d) El-Hendawy, A. M.; Griffith, W. P.; O'Mahoney, C. A.; Williams, D. J. *Polyhedron* **1989**, *8*, 519. (e) Kabanos, T. A.; Slawin, A. M. Z.; Williams, D. J. *Polyhedron* **1992**, *11*, 995. (f) Albrecht, M.; Franklin, S. J.; Raymond, K. N. *Inorg. Chem.* **1994**, *33*, 5785. (g) Sinclair, L.; Mondal, J. U.; Uhrhammer, D.; Schultz, F. A. *Inorg. Chim. Acta* **1998**, *278*, 1.
(2) Pierpont, C. G.; Buchanan, R. M. *J. Am. Chem. Soc.* **1975**, *97*, 4912.
(3) Pierpont, C. G.; Buchanan, R. M. *J. Am. Chem. Soc.* **1975**, *97*, 6450.
(4) Buchanan, R. M.; Pierpont, C. G. *Inorg. Chem.* **1979**, *18*, 1616.
(5) (a) Wilshire, J. P.; Leon, L.; Bosserman, P.; Sawyer, D. T. *J. Am. Chem. Soc.* **1979**, *101*, 3379. (b) Wilshire, J. P.; Leon, L.; Bosserman, P.; Sawyer, D. T.; Buchanan, R. M.; Pierpont, C. G. In *Third International Conference on the Chemistry and Uses of Molybdenum*; Barry, H. F., Mitchell, P. C. H., Eds.; Climax Molybdenum Co.: Ann Arbor, 1979; p 264. (c) Wilshire, J. P.; Leon, L.; Bosserman, P.; Sawyer, D. T. In *Molybdenum Chemistry of Biological Significance*; Newton, W. E., Otsuka, S., Eds.; Plenum Press: New York, 1980; p 327. (d) Lim, M.-C.; Sawyer, D. T. *Inorg. Chem.* **1982**, *21*, 2839. (e) Sawyer, D. T.; Tsuchiya, T.; Po, H. N.; Pham, K. Q. In *Fourth International Conference on the Chemistry and Uses of Molybdenum*; Barry, H. F., Mitchell, P. C. H., Eds.; Climax Molybdenum Co.: Golden, CO, 1982; p 107.
(6) Cass, M. E.; Pierpont, C. G. *Inorg, Chem.* **1986**, *25*, 122.
(7) Pierpont, C. G.; Buchanan, R. M. *Inorg. Chem.* **1982**, *21*, 652.
(8) Prokof'ev, A. I.; Vol'eva, V. B.; Prokof'eva, T. I.; Bubnov, N. N.; Solodovnikov, S. P.; Erahov, V. V.; Kabachnik, M. I. *Dokl. Akad. Nauk SSSR (Engl.)* **1988**, *300*, 179.
(9) Lange, C. W.; Conklin, B. J.; Pierpont, C. G. *Inorg. Chem.* **1994**, *33*, 1276.
(10) Part of this research appeared earlier in the form of a communication. Liu, C.-M.; Restorp, P.; Nordlander, E.; Pierpont, C. G. *Chem. Commun.* **2001**, 2686.
(11) Belostotskaya, I. S.; Komissarova, N. L.; Dzhuaryan, E. V.; Ershov, V. V. *Isv. Akad. Nauk SSSR* **1984**, 1610.

[Mo(O-^{i}Pr)$_2$(3,6-DBCat)$_2$]: ^{1}H NMR (300 MHz, $CDCl_3$, ppm) 6.590 (s, 2H$_{ring}$), 5.733 (p, 1H^{i}PrO), 1.474 (s, 9H$_{Bu}$), 1.454 (s, 9H$_{Bu}$), 1.199 (m, 6H^{i}PrO); UV−vis ($CHCl_3$, λ_{max}(nm)) 273 (17.9×10^3 $M^{-1}cm^{-1}$), 443 (8.52×10^3), 616 (6.33×10^3); IR (KBr, cm^{-1}): 1591 (w), 1487 (m), 1441 (w), 1385 (s), 1357 (m), 1331 (w),1316 (m), 1287 (w), 1202 (w), 1165 (w), 1127 (w), 1109 (s), 1100 (s), 1031 (w), 977 (vs), 964 (vs), 856 (s), 814 (m), 807 (m), 705 (s); FAB$^+$-MS (*m*/*z*) 656 [Mo(*i*-PrO)$_2$(3,6-DBCat)$_2^+$], 554 [MoO(3,6-DBCat)$_2^+$].

***cis*-[MoO(dmso)(3,6-DBCat)$_2$]. Method 1.** 3,6-DBBQ (0.132 g, 0.6 mmol) and [Mo(CO)$_6$] (0.079 g, 0.3 mmol) were refluxed in toluene (50 mL) under N_2 for 20 h. The solution was cooled to room temperature and reduced in volume to approximately 30 mL, and DMSO (2−3 mL) was added under N_2. The volume of the solution was reduced further under a flow of N_2, and dark crystals of [MoO(dmso)(3,6-DBCat)$_2$] formed in 72% yield. Crystals of the complex obtained by this procedure were found to be unsolvated. However, when obtained from a solution containing excess DMSO, crystals of the complex formed as the DMSO solvate, [MoO(dmso)-(3,6-DBCat)$_2$]·DMSO.

Method 2. [{MoO(3,6-DBCat)$_2$}$_4$] (250 mg) was dissolved in toluene (30 mL), and 1 mL of DMSO was added to the solution. The solution was heated at reflux for 3 h, and reduced in volume. Crystals of [MoO(dmso)(3,6-DBCat)$_2$] were obtained in approximately quantitative yield. However, if the solution containing [{MoO(3,6-DBCat)$_2$}$_4$] and DMSO was maintained at room temperature without heating, the reaction time for complete conversion to [MoO(dmso)(3,6-DBCat)$_2$] was greater than 1 month.

[MoO(dmso)(3,6-DBCat)$_2$]: ^{1}H NMR (300 MHz, $CDCl_3$, 18 °C, ppm) 6.58 (s, 4H$_{ring}$), 2.925 (s, 6H$_{DMSO}$), 1.215 (s, 36H$_{Bu}$); ^{1}H NMR (300 MHz, CD_2Cl_2, −98 °C, ppm) 6.62 (1, H$_{ring}$), 6.59 (1, H$_{ring}$), 6.54 (1, H$_{ring}$), 6.45 (1, H$_{ring}$), 3.05 (3, H$_{DMSO}$), 2.81 (3, H$_{DMSO}$), 1.29 (18, H$_{Bu}$), 0.99 (9, H$_{Bu}$), 0.83 (9, H$_{Bu}$); UV−vis ($CHCl_3$, λ_{max}(nm)) 274 (12.8×10^3 M^{-1} cm^{-1}), 456 (6.5×10^3); IR (KBr, cm^{-1}) 1630 (m), 1575 (m), 1482 (m), 1467 (w), 1392 (m), 1358 (m), 1273 (w), 1241 (w), 1200 (s), 1179 (w), 1125 (m), 1028 (s), 984 (s), 952 (m), 925 (s), 812 (w), 802 (w), 716 (s); FAB$^+$-MS (*m*/*z*) 632 [MoO(dmso)(3,6-DBCat)$_2^+$], 554 [MoO(3,6-DBCat)$_2^+$].

***cis*-[MoO(OAsPh$_3$)(3,6-DBCat)$_2$].** 3,6-DBBQ (0.132 g, 0.6 mmol) and [Mo(CO)$_6$] (0.079 g, 0.3 mmol) were refluxed in toluene (50 mL) under N_2 for 20 h. The solution was cooled to room temperature, and triphenylarsine oxide (97 mg, 0.3 mmol) dissolved in 20 mL of toluene was added under N_2. The color of the solution slowly turned to a deep red-brown. The solvent was evaporated under a flow of N_2, and crystals of [MoO(OAsPh$_3$)(3,6-DBCat)$_2$] were obtained in 80% yield as a toluene solvate.

[MoO(OAsPh$_3$)(3,6-DBCat)$_2$]: ^{1}H NMR (300 MHz, $CDCl_3$, 20 °C, ppm) 7.845(s, 3H$_{Ph3AsO}$), 7.820(s, 3H$_{Ph3AsO}$), 7.654(t, 3H$_{Ph3AsO}$), 7.539(s, 3H$_{Ph3AsO}$), 7.355(s, 3H$_{Ph3AsO}$), 6.499 (s, 4H$_{ring}$), 1.166 (s, 36H$_{Bu}$); UV−vis ($CHCl_3$, λ_{max}(nm)) 271 (15.5×10^3 M^{-1} cm^{-1}), 352 (4.6×10^3), 480 (6.1×10^3); IR (KBr, cm^{-1}) 1574 (w), 1483 (m), 1463 (w), 1441 (s), 1384 (vs), 1358 (s), 1343 (m), 1311 (w), 1272 (w), 1245 (m), 1201 (m), 1181 (w), 1125 (w), 1087 (m), 1028 (w), 997 (w), 985 (s), 916 (vs), 829 (s), 811 (s), 799 (m), 740 (s), 714 (s); FAB$^+$-MS (*m*/*z*) 876 [MoO(OAsPh$_3$)(3,6-DBCat)$_2^+$], 554 [MoO(3,6-DBCat)$_2^+$].

***cis*-[MoO(py-O)(3,6-DBCat)$_2$].** 3,6-DBBQ (0.132 g, 0.6 mmol) and [Mo(CO)$_6$] (0.079 g, 0.3 mmol) were refluxed in toluene (50 mL) under N_2 for 20 h. The solution was cooled to room temperature, and pyridine *N*-oxide (29 mg, 0.3 mmol) dissolved in 10 mL of toluene was added under N_2. The color of the solution slowly turned to a deep purple. The solvent was evaporated under a flow of N_2, and crystals of [MoO(py-O)(3,6-DBCat)$_2$] were obtained in 86% yield.

[MoO(py-O)(3,6-DBCat)$_2$]: ^{1}H NMR (300 MHz, $CDCl_3$, 20 °C, ppm) 8.766(d, 1H$_{Py}$), 8.226(s, 1H$_{Py}$), 7.955(t, 1H$_{Py}$), 7.689(t, 1H$_{Py}$), 7.285(s, 1H$_{Py}$), 6.499 (s, 4H$_{ring}$), 1.166 (s, 36H$_{Bu}$); UV−vis ($CHCl_3$, λ_{max}(nm)) 275 (15.7×10^3 M^{-1} cm^{-1}), 513 (2.0×10^3); IR (KBr, cm^{-1}) 1475 (s), 1392 (m), 1379 (w), 1358 (w), 1341 (w), 1242 (s), 1201 (m), 1172 (s), 983 (s), 929 (s), 814 (w), 804 (4), 723 (s), 715 (s); FAB$^+$-MS (*m*/*z*) 649 [MoO(PyO)(3,6-DBCat)$_2^+$], 554 [MoO-(3,6-DBCat)$_2^+$].

[CoCp$_2$][MoO(3,6-DBCat)$_2$]. Cobaltocene (76 mg, 0.4 mmol) was dissolved in 50 mL of CH_2Cl_2, and added to [MoO(dmso)-(3,6-DBCat)$_2$] (142 mg, 0.2 mmol) dissolved in 30 mL CH_2Cl_2 under N_2. The solution immediately turned red-orange. The solvent was removed under a flow of N_2, giving a dark brown precipitate. The precipitate was redissolved in a minimum quantity of CH_2Cl_2 and condensed in volume, and 5 mL of acetonitrile was layered on the solution to promote crystallization. Orange crystals of [CoCp$_2$]-[MoO(3,6-DBCat)$_2$] were obtained in 95% yield as a mixed dichloromethane/acetonitrile solvate.

[CoCp$_2$][MoO(3,6-DBCat)$_2$]: EPR (CH_2Cl_2) $\langle g_{iso} \rangle = 1.903$, $a(^{95,97}\text{Mo}) = 44 \times 10^{-4}$ cm^{-1}; UV−vis (CH_2Cl_2, λ_{max}(nm)) 406 (5.8×10^4 M^{-1} cm^{-1}); IR (KBr, cm^{-1}) 1625 (bw), 1492 (s), 1452 (m), 1411 (vs), 1401 (vs), 1384 (vs), 1365 (m), 1268 (m), 1248 (m), 1203 (w), 1142 (w), 1028 (w), 1011 (w), 988 (m), 954 (m), 926 (s), 863 (m), 812 (w), 793 (w), 712 (m); FAB$^-$-MS (*m*/*z*) 554 [MoO(3,6-DBCat)$_2^-$].

Crystal Structure Determinations. Intensity measurements were made using either a Siemens P4 diffractometer ([{MoO(3,6-DBCat)$_2$}$_4$], [MoO(dmso)(3,6-DBCat)$_2$]·DMSO, [CoCp$_2$][MoO(3,6-DBCat)$_2$]·0.5CH_2Cl_2·0.5CH_3CN) or a Siemens SMART CCD diffractometer ([MoO(py-O)(3,6-DBCat)$_2$], [Mo(O-^{i}Pr)$_2$(3,6-DB-Cat)$_2$], [MoO(Ph$_3$AsO)(3,6-DBCat)$_2$]·1.5C_7H_8). Descriptions of the procedures used for data collection, structure solution, and refinement are contained in CIFs, and a summary of crystallographic parameters is given in Table 1. Structure solution and refinement was routine for all six structure determinations. All data were collected using Mo Kα radiation with a wavelength of 0.71073 Å. Discrepancy indices are defined as $R = \sum||F_o| - |F_c||/\sum|F_o|$ and $R_w = [\sum w(|F_o| - |F_c|)^2/\sum w(F_o)^2]^{1/2}$. In cases where there were solvate molecules, solvent atom locations were obtained from a difference Fourier map calculated with phases from the complete complex molecule. All calculations were carried out using programs contained in the SHELXTL library of crystallographic computer programs.

Results

The coordination chemistry of metals of the first transition series with quinone ligands has been frequently concerned with complexes containing radical *o*-semiquinonate ligands.[12] In contrast, related complexes prepared with metals of the second and third transition series contain metal ions in high oxidation states coordinated by catecholate dianions.[13] Complexes of the Cr, Mo, W triad were among the first group of metals to show this pattern in charge distribution with ligands derived from tetrachloro-1,2-benzoquinone (Cl_4BQ). The neutral complex of chromium obtained by reacting Cl_4BQ with $Cr(CO)_6$ has been shown to be [$Cr^{III}(Cl_4SQ)_3$], and the

(12) Pierpont, C. G.; Attia, A. S. *Collect. Czech. Chem. Commun.* **2001**, *66*, 33.
(13) Pierpont, C. G. *Coord. Chem. Rev.* **2001**, *219*−*221*, 415.

Table 1. Crystallographic Data for [{Mo(μ-O)(3,6-DBCat)$_2$}$_4$], *cis*-[Mo(O-^{i}Pr)$_2$(3,6-DBCat)$_2$], (CoCp$_2$)[MoO(3,6-DBCat)$_2$], *cis*-[MoO(dmso)(3,6-DBCat)$_2$], *cis*-[MoO(O-py)(3,6-DBCat)$_2$], and *cis*-[MoO(OAsPh$_3$)(3,6-DBCat)$_2$]

	[Mo(μ-O)-(3,6-DBCat)$_2$]$_4$	Mo(O-^{i}Pr)$_2$-(3,6-DBCat)$_2$	(CoCp$_2$)[MoO(3,6-DBCat)$_2$]·0.5CH$_2$Cl$_2$·0.5CH$_3$CN	MoO(dmso)-(3,6-DBCat)$_2$·DMSO	MoO(O-py)-(3,6-DBCat)$_2$	MoO(OAsPh$_3$)-(3,6-DBCat)$_2$·1.5C$_7$H$_8$
formula	$C_{14}H_{20}Mo_{0.5}O_{2.5}$	$C_{34}H_{54}MoO_6$	$C_{39.5}H_{52.5}CoMoClN_{0.5}O_5$	$C_{32}H_{52}MoO_7S_2$	$C_{33}H_{45}MoNO_6$	$C_{58}H_{70}MoAsO_6$
fw	276.27	654.71	809.11	708.8	647.64	1034
cryst syst	tetragonal	monoclinic	monoclinic	triclinic	triclinic	monoclinic
space group	*P*4/*nnc*	*C*2/*c*	*P*2$_1$/*c*	$P\bar{1}$	$P\bar{1}$	*P*2$_1$/*c*
Z	16	4	4	2	2	4
a, Å	22.5679(15)	11.1595(2)	13.0347(2)	10.6946(1)	10.3400(1)	16.6888(5)
b, Å	22.5679(15)	29.0306(6)	15.1104(2)	11.2383(1)	10.6052(3)	17.5638(5)
c, Å	13.0099(12)	11.8944(2)	20.1387(1)	16.6845(1)	17.1703(3)	19.6028(6)
α, deg	90	90	90	99.523(1)	82.243(1)	90
β, deg	90	116.703(1)	105.801(1)	93.247(1)	76.346(1)	109.806(1)
γ, deg	90	90	90	114.664(1)	60.842(1)	90
V, Å^3	6626.1(9)	3442.4(1)	3816.63(8)	1779.48(3)	1597.35(6)	5406.0(3)
T, K	293(2)	144(2)	293(2)	142(2)	154(2)	143(2)
d, g cm^{-3}	1.108	1.263	1.408	1.323	1.347	1.27
μ, mm^{-1}	0.424	0.421	0.877	0.527	0.454	0.897
R (R_w)	0.0584 (0.1878)	0.0316 (0.0869)	0.0417 (0.1063)	0.0513 (0.1090)	0.0507 (0.1193)	0.0435 (0.0958)
GOF	1.373	1.018	1.031	1.04	1.03	1.025

temperature-dependent magnetic properties of the complex show the effects of antiferromagnetic coupling between the $S = {}^3/_2$ metal ion and the three radical ligands.[14] Related reactions carried out with [Mo(CO)$_6$] or [W(CO)$_6$] were found to give the [{M^{VI}(Cl$_4$Cat)$_3$}$_2$] (M = Mo, W) dimers.[15] Differences in the structural features of the quinone ligands of [Cr^{III}(Cl$_4$SQ)$_3$] and the [{M^{VI}(Cl$_4$Cat)$_3$}$_2$] dimers pointed to the difference in charge distribution, and the differences in the features of catecholate and semiquinonate ligands have proven to be a reliable method of assigning charge distribution in subsequent complexes prepared with quinone ligands.[13] The complexes of molybdenum were among the earliest well-characterized examples of catecholate coordination,[16] and reactions between [Mo(CO)$_6$] and benzoquinone in a hydrocarbon solvent have been found to be useful in providing control of reaction conditions. However, the reaction carried out with 3,5-di-*tert*-butyl-1,2-benzoquinone was found to show an unusual sensitivity to trace quantities of dioxygen in the reaction medium.[6] Reactions carried out under scrupulously oxygen-free conditions were found to form initially [Mo^{VI}(3,5-DBCat)$_3$], which reacted further with dioxygen to give the [{MoO(3,5-DBCat)$_2$}$_2$] dimer. This product has also been obtained by treating MoO$_3$ or [MoO$_2$-(acac)$_2$] with 3,5-di-*tert*-butylcatechol, and the 3,5-DBCat ligand has shown no tendency to give the [MoO$_2$(Cat)$_2$]$^{2-}$ dianion formed commonly with catecholate ligands containing substituents that are less strongly electron releasing than the tertiary butyl group.[5] The extreme oxygen sensitivity of [Mo(3,5-DBCat)$_3$] is in sharp contrast with the resistance of [{MoO(3,5-DBCat)$_2$}$_2$] toward the addition of a second oxo ligand.

Structural characterization on [{MoO(3,5-DBCat)$_2$}$_2$] has shown that the adjacent metal ions are bridged by oxygen atoms at the 1-ring position of the catecholate ligands (Figure 1).[4] This is the oxygen atom adjacent to a ring carbon atom that has a C−H bond, rather than a bulky *tert*-butyl group, and this oxygen has been found to commonly bridge metal ions in its coordination to metals with the ligand in the form of either a catecholate or a semiquinonate. To block bridging interactions, and to eliminate the possibility of structural isomers that may form with 3,5-DBCat, we have used 3,6-di-*tert*-butyl-1,2-benzoquinone (3,6-DBBQ) in recent studies on Cat and SQ coordination.[9,10]

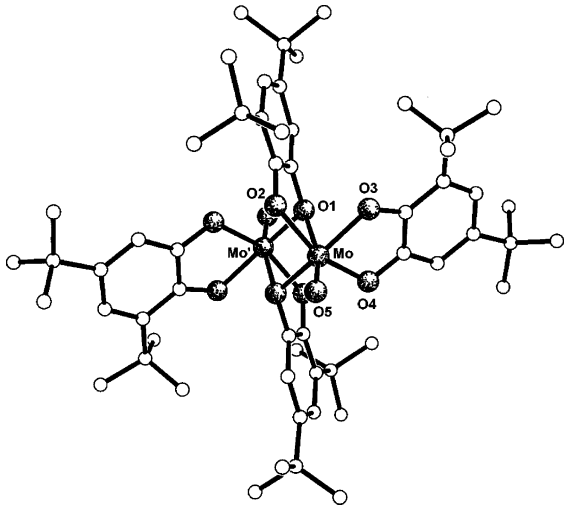

Figure 1. View of the [{MoO(3,5-DBCat)$_2$}$_2$] dimer showing bridging interactions for the catecholate oxygens at the 1-ring position of 3,5-di-*tert*-butylcatechol (ref 4).

Reaction between [Mo(CO)$_6$] and 3,6-Di-*tert*-butyl-1,2-benzoquinone. The presence of *tert*-butyl substituents at ring carbon atoms adjacent to both quinone oxygen atoms eliminates the possibility of forming a dimer that is similar in structure to [{MoO(3,5-DBCat)$_2$}$_2$]. Instead, it was thought that a 5-coordinate monomeric product, [MoO(3,6-DBCat)$_2$], might form as the exclusive product. This monomer might be similar in structure to trigonal bipyramidal [MoO{OC-(CF$_3$)$_3$}$_4$] with an equatorial oxo ligand.[17] ^{1}H NMR spectra

(14) (a) Pierpont, C. G.; Downs, H. H. *J. Am. Chem. Soc*. **1976**, *98*, 4834. (b) Buchanan, R. M.; Kessel, S. L.; Downs, H. H.; Pierpont, C. G.; Hendrickson, D. N. *J. Am. Chem. Soc*. **1978**, *100*, 7894.

(15) (a) Pierpont, C. G.; Downs, H. H. *J. Am. Chem. Soc*. **1975**, *97*, 2123. (b) deLearie, L. A.; Haltiwanger, R. C.; Pierpont, C. G. *Inorg. Chem*. **1988**, *27*, 3842.

(16) Tkachev, V. V.; Atovmyan, L. O. *Koord. Khim*. **1975**, *1*, 845.

(17) Johnson, D. A.; Taylor, J. C.; Waugh, A. B. *J. Inorg. Nucl. Chem*. **1980**, *42*, 1271.

recorded on the crude dark blue-violet product obtained from the reaction between [$Mo(CO)_6$] and 3,6-DBBQ showed multiple resonances in the *tert*-butyl region indicating a mixture of products. Chromatographic separation gave two distinct fractions in roughly equal proportions. The fraction obtained at lower R_f appeared to consist of a mixture of products (from ^{1}H NMR). Mass spectral analysis (EI) of this fraction provided Mo isotope patterns for two complex ions. Peaks in the 552−554 mass region fit the pattern expected for the [$MoO(3,6\text{-}DBCat)_2]^+$ ion that might result from fragmentation of [$\{MoO(3,6\text{-}DBCat)_2\}_n$] oligomers. A second major component of this fraction gave peaks in the 756−758 region that could be modeled as the [$Mo(3,6\text{-}DBCat)_3]^+$ ion. From experience with related 3,5-DBBQ reactions, it is not unreasonable to expect that [$Mo(3,6\text{-}DBCat)_3$] would be formed as a product of the [$Mo(CO)_6$]/3,6-DBBQ reaction.

^{1}H NMR analysis on the fraction obtained at higher R_f gave a less complicated result. Two resonances appeared in the *tert*-butyl region at 0.947, 0.997 ppm, and one resonance appeared in the aromatic region at 6.45 ppm, and mass spectral analysis also gave a pattern for the [$MoO(3,6\text{-}DBCat)_2]^+$ ion. Slow evaporation of the solvent combination used in the chromatographic separation gave single crystals of the complex obtained in this fraction.

[$\{MoO(3,6\text{-}DBCat)_2\}_4$]. Preliminary investigation of crystals obtained from the high R_f fraction indicated that they formed in the tetragonal crystal system. Solution of the structure revealed that the complex molecule was located at the intersection of 2-fold axes at a position of 4-fold symmetry in space group *P*4/*nnc*. The structure consists of one independent 3,6-DBCat ligand chelated to a Mo atom located on one 2-fold axis. A crystallographic 2-fold axis passing through the metal generates a second 3,6-DBCat ligand chelated to the Mo. Crystallographic 4-fold symmetry generates three additional [$Mo(3,6\text{-}DBCat)_2$] fragments, with the four Mo centers forming corners of a perfect square. Bridging oxo ligands are located on 2-fold axes directed between the locations of two Mo atoms, linking metal atoms along sides of the square. A view of the tetramer is given in Figure 2, and bond distances and angles are listed in Table 2.

Each of the Mo centers, of local C_2 symmetry, is optically active, and the 4-fold symmetry of the square requires the same optical symmetry at each of the metal atoms of the tetramer. Translational symmetry along the 4-fold axis generates columns of squares of the same chirality in the crystal structure. Crystallographic inversion centers between columns generate adjacent columns of opposite chirality. Consequently, the crystal structure consists of parallel columns of ΔΔΔΔ and ΛΛΛΛ isomers of [$\{MoO(3,6\text{-}DBCat)_2\}_4$] as shown in Figure 3 formed as the product of enantioselective self-assembly.[18] The disposition of *tert*-butyl groups about the upper surface of the square (Figure 2) appears to make adjacent centers of opposite chirality sterically unfavorable in the closed structure. It is certainly possible that adjacent Mo centers of opposite chirality may link through oxo bridges, and this may lead to open oligomers obtained in the low R_f fraction from the reaction mixture. Condensation to form either the square tetramer or a linear oligomer points to the formation of the [$MoO(3,6\text{-}DBCat)_2$] monomer as the initial product of the reaction between [$Mo(CO)_6$] and 3,6-DBBQ in the presence of trace quantities of dioxygen.

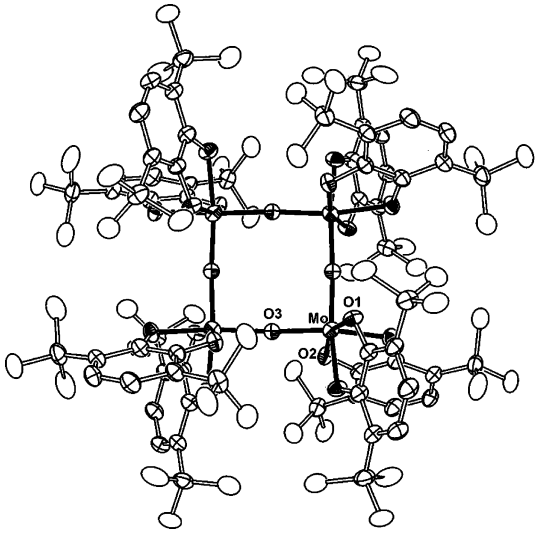

Figure 2. View of the ΛΛΛΛ-[$\{Mo(\mu\text{-}O)(3,6\text{-}DBCat)_2\}_4$] chiral square down the tetragonal 4-fold axis.

Table 2. Bond Lengths (Å) and Angles (deg) for [$\{Mo(\mu\text{-}O)(3,6\text{-}DBCat)_2\}_4$], *cis*-[$Mo(O\text{-}^i Pr)_2(3,6\text{-}DBCat)_2$], and the [$MoO(3,6\text{-}DBCat)_2]^-$ Anion[a]

	[$Mo(\mu$-O)-(3,6-DBCat)$_2]_4$	Mo(O-^{i}Pr)$_2$-(3,6-DBCat)$_2$	[MoO-(3,6-DBCat)$_2]^-$
Mo−O1	1.929(3)	1.955(1)	1.987(2)
Mo−O2	1.993(3)	1.968(1)	1.968(2)
Mo−O3	1.8761(4)	1.848(1)	1.690(2)
C−O1	1.347(5)	1.358(2)	1.364(3)
C−O2	1.344(5)	1.346(2)	1.369(3)
O1−Mo−O3	108.6(1)	84.81(4)	109.41(7)
O2−Mo−O3	93.3(1)	91.59(5)	110.61(7)
O3−Mo−O3′	93.5(2)	96.32(7)	87.26(6)

[a] Lengths and angles to O1 and O2 in the table are averaged values to O1, O4 and O2, O3 of {[$MoO(3,6\text{-}DBCat)_2]^-$} in Figure 10. Values to O3 in the table are to apical oxygen O5 in Figure 10.

***cis*-[Mo(O-^{i}Pr)$_2$(3,6-DBCat)$_2$].** An attempted recrystallization of a crude sample of [$\{MoO(3,6\text{-}DBCat)_2\}_4$] from hexane was observed to change color upon addition of a small quantity of *i*-propanol to promote crystallization. The dark blue-violet hexane solution of [$\{MoO(3,6\text{-}DBCat)_2\}_4$] became dark purple. Slow evaporation of the solvent gave crystals of the purple product. Crystallographic characterization indicated that it was the bis(*iso*-propoxo) complex *cis*-[$Mo^{VI}(O\text{-}^i Pr)_2(3,6\text{-}DBCat)_2$]. A view of the molecule is shown in Figure 4; bond distances and angles are given in Table 2. The coordination geometry and bond lengths to the metal are similar to those of [$\{MoO(3,6\text{-}DBCat)_2\}_4$], but with propyl groups bonded to the oxygens that would bridge to adjacent metals in the tetramer. The formation of this product from a reaction that must take place by hydrolysis of the oxo ligand of [$MoO(3,6\text{-}DBCat)_2$] is quite surprising. It

(18) Ziegler, M.; Davis, A. V.; Johnson, D. W.; Raymond, K. N. *Angew. Chem., Int. Ed.* **2003**, *42*, 665.

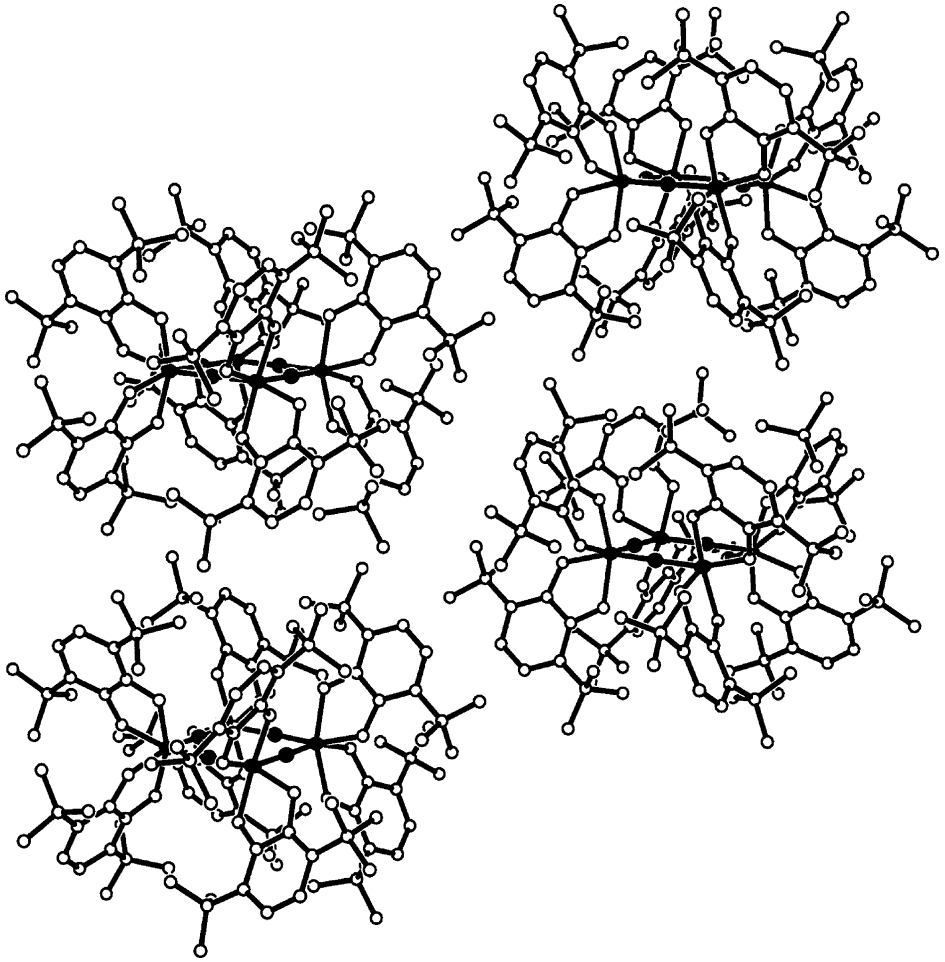

Figure 3. Parallel columns of ΛΛΛΛ-[{Mo(μ-O)(3,6-DBCat)$_2$}$_4$] and ΔΔΔΔ-[{Mo(μ-O)(3,6-DBCat)$_2$}$_4$] tetramers in the crystal structure of [{Mo(μ-O)(3,6-DBCat)$_2$}$_4$].

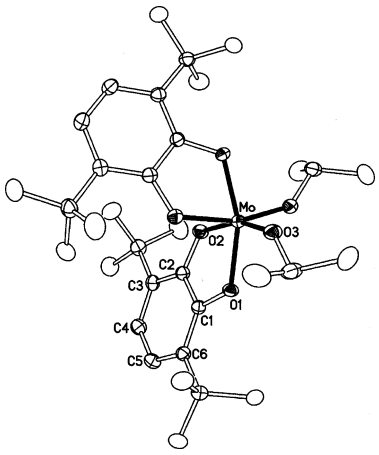

Figure 4. View of *cis*-[Mo(O-^{i}Pr)$_2$(3,6-DBCat)$_2$]. The molecule is located along a crystallographic 2-fold axis that bisects the angle formed by the isopropoxide ligands at the Mo.

implies that the oxo ligand coordinated to the Mo(VI) center is a stronger base than the isopropoxide ion. This must occur as a consequence of strong σ and π donation from the catecholate oxygen atoms. ^{1}H NMR spectra recorded on the complex show two resonances in the tertiary butyl region, consistent with the cis structure of the molecule, indicating that the complex is stereochemically rigid in solution at room temperature.

Studies on the Addition of Oxygen-Atom Donors to [MoO(3,6-DBCat)$_2$]. Catalytic oxygen-atom transfer reactions involving Mo(VI) are associated with processes of biological and industrial importance.[19,20] Focusing specifically on bioinorganic reactions catalyzed by molybdoenzymes of the DMSO reductase family, it has been of interest to investigate the coordination of substrate ligands that may potentially serve as oxygen-atom donors to [MoO(3,6-DBCat)$_2$]. The Mo center of the dmso reductase class of enzymes is coordinated by two bidentate pyranopterin dithiolene ligands (S-S), and, at the outset of this project, the metal was thought to oscillate between [Mo^{VI}O$_2$(S-S)$_2$] and [Mo^{IV}O(S-S)$_2$] species with oxidation (or reduction) of substrate.[21] Structural characterization on a reduced form of the enzyme containing a dmso substrate molecule coordinated to the metal showed that addition occurred at a coordination site cis to the oxo ligand of the reduced metal.[21a] More recent structural characterization has concluded that the oxo ligand thought to be present in the [Mo^{IV}O(S-S)$_2$] species is an artifact resulting from structural disorder of the Mo atom,

(19) Hille, R. *Chem. Rev.* **1996**, *96*, 2757.
(20) Sheldon, R. A. In *Applied Homogeneous Catalysis with Organometallic Compounds*; Cornils, B., Hermann, W. A., Eds.; VCH Publishers: Weinheim, 1996; p 411.
(21) (a) McAlpine, A. S.; McEwan, A. G.; Bailey, S. *J. Mol. Biol.* **1998**, *275*, 613. (b) George, G. N.; Hilton, J.; Temple, C.; Prince, R. C.; Rajagopalan, K. V. *J. Am. Chem. Soc.* **1999**, *121*, 1256.

and that changes at the active site involve [$Mo^{VI}O(S\text{-}S)_2$(O-ser)] and [$Mo^{IV}(S\text{-}S)_2$(O-ser)] species.[22] The results of oxidized substrate addition reactions described below, nevertheless, remain pertinent to interests in oxo transfer chemistry to Mo(VI).

With the potential stability of the [$Mo^{VI}O$(3,6-DBCat)$_2$] monomer in dilute solutions, it became of interest to see if reductively induced oxo transfer to the metal might be observed in a process that does not require a change in oxidation state at the Mo (eq 4). The product of the reaction

$$Mo^{VI}O(3,6\text{-DBCat})_2 + \text{O-Subst} + 2e^- \rightarrow [\textit{cis}\text{-}Mo^{VI}O_2(3,6\text{-DBCat})_2]^{2-} + \text{Subst} \quad (4)$$

would be a *cis*-dioxomolybdenum(VI) species of the type found commonly in the coordination chemistry of molybdenum with catecholate ligands that do not contain two *tert*-butyl substituents.[23]

***cis*-[MoO(dmso)(3,6-DBCat)$_2$].** The addition of dmso to a dilute, freshly prepared solution of [MoO(3,6-DBCat)$_2$] gave an immediate color change to that of the addition product, [MoO(dmso)(3,6-DBCat)$_2$]. Addition of dmso to a more concentrated solution containing a mixture of {MoO-(3,6-DBCat)$_2$}$_n$ oligomers, including the [{MoO(3,6-DBCat)$_2$}$_4$] tetramer, required hours for complete conversion to the addition product. When isolated in crystalline form from toluene or hexane solutions, the complex is unsolvated. However, samples obtained from a solution containing excess dmso form as the solvate, [MoO(dmso)(3,6-DBCat)$_2$]·DMSO. Crystalline samples of the complex in both the solvated and unsolvated forms have been investigated crystallographically.[10] In both structure determinations features of the complex molecule are the same. The result obtained for the dmso solvate is of slightly higher precision and will be described herein. A view of the dmso addition product is shown in Figure 5. The coordinated dmso molecule is bonded to the Mo at a site cis to the oxo ligand. Selected bond lengths and angles are given for [MoO(dmso)-(3,6-DBCat)$_2$]·DMSO in Table 3.

It is perhaps surprising that, as a relatively weak donor, the dmso ligand bonds at a site adjacent to the oxo ligand, with a catecholate oxygen occupying the coordination site trans to the oxo oxygen. The catecholate oxygens are strong σ and π donors, as is the oxo oxygen. The structure is significant in placing the dmso oxygen at a site poised to give a *cis*-dioxomolybdenum(VI) species with release of dimethyl sulfide upon two-electron reduction (eq 4).[24] At room temperature the ^{1}H NMR spectrum of [MoO(dmso)-(3,6-DBCat)$_2$] consists of three resonances: one each for the ring and *tert*-butyl protons of the 3,6-DBCat ligands and a third for the dmso ligand. The stereodynamic effect responsible for time-averaging proton resonances will be described below.

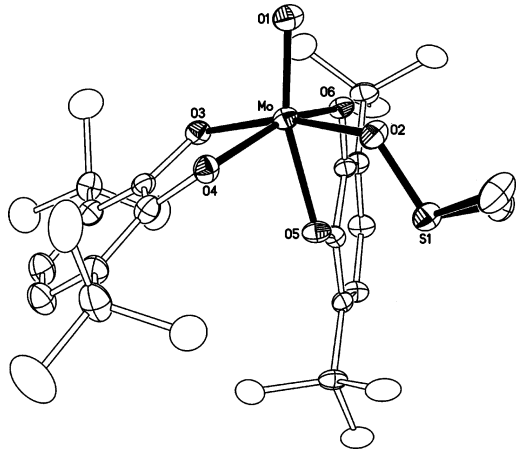

Figure 5. View showing the cis coordination of dmso in *cis*-[MoO(dmso)-(3,6-DBCat)$_2$].

Table 3. Selected Bond Lengths (Å) and Angles (deg) for the Products of Substrate Oxide Addition to [MoO(3,6-DBCat)$_2$]

	MoO(dmso)-(3,6-DBCat)$_2$	MoO(O-py)-(3,6-DBCat)$_2$	MoO(OAsPh$_3$)-(3,6-DBCat)$_2$
Mo−O1	1.694(2)	1.691(2)	1.701(2)
Mo−O2	2.084(2)	2.089(2)	2.051(2)
Mo−O3	1.960(2)	1.954(2)	1.968(2)
Mo−O4	1.951(2)	1.946(2)	1.947(2)
Mo−O5	2.077(2)	2.071(2)	2.071(2)
Mo−O6	1.954(2)	1.939(2)	1.944(2)
C−O3	1.363(4)	1.352(3)	1.358(3)
C−O4	1.365(4)	1.360(3)	1.379(3)
C−O5	1.326(4)	1.317(3)	1.318(3)
C−O6	1.347(4)	1.335(3)	1.351(3)
O2−X	1.565(2)	1.378(3)	1.693(2)
O1═Mo−O2	89.16(10)	90.23(10)	91.84(7)
O1═Mo−O3	104.13(10)	104.80(11)	101.04(8)
O1═Mo−O4	109.21(11)	107.80(10)	109.00(8)
O1═Mo−O6	91.89(10)	91.43(10)	91.72(8)

***cis*-[MoO(py-O)(3,6-DBCat)$_2$].** The addition of pyridine *N*-oxide to [MoO(3,6-DBCat)$_2$] is accompanied by a change in color of the solution to a deep purple. Slow evaporation of a toluene solution of the addition product gave crystals suitable for crystallographic analysis. A view of the [MoO-(py-O)(3,6-DBCat)$_2$] molecule is shown in Figure 6, and selected bond lengths are given in Table 3. As in the case of [MoO(dmso)(3,6-DBCat)$_2$], the pyridine *N*-oxide ligand is coordinated at a site cis to the terminal oxo ligand. Metrical values to the metal are similar to the dmso addition product, and general structural features of the inner coordination sphere are similar for the two compounds. ^{1}H NMR spectra recorded at room temperature show five separate resonances for the ring protons of the pyridine ring, but the catecholate ring and *tert*-butyl protons appear as single, time averaged peaks at 6.50 and 1.166 ppm as the result of a dynamic exchange process.

***cis*-[MoO(OAsPh$_3$)(3,6-DBCat)$_2$].** Addition of either triphenylphosphine oxide or triphenylarsine oxide to a solution containing [MoO(3,6-DBCat)$_2$] resulted in a color change to dark red-brown as an indication of immediate adduct

(22) (a) Li, H.-K.; Temple, C.; Rajagopalan, K. V.; Schindelin, H. *J. Am. Chem. Soc.* **2000**, *122*, 7673. (b) Bray, R. C.; Adams, B.; Smith, A. T.; Benett, B.; Bailey, S. *Biochemistry* **2000**, *39*, 11258.

(23) (a) Kustin, K.; Liu, S.-T. *J. Am. Chem. Soc.* **1973**, *95*, 2487. (b) Charney, L. M.; Finklea, H. O.; Schultz, F. A. *Inorg. Chem.* **1982**, *21*, 549. (c) Griffith, W. P.; Nogueira, H. I. S.; Parkin, B. C.; Sheppard, R. N.; White, A. J. P.; Williams, D. J. *J. Chem. Soc., Dalton Trans.* **1995**, 1775. (d) Duhme, A.-K.; Dauter, Z.; Hider, R. C.; Pohl, S. *Inorg. Chem.* **1996**, *35*, 3059. (e) Duhme, A.-K.; Davies, S. C.; Hughes, D. L. *Inorg. Chem.* **1998**, *37*, 5380.

(24) Thapper, A.; Deeth, R. J.; Nordlander, E. *Inorg. Chem.* **2002**, *41*, 6695.

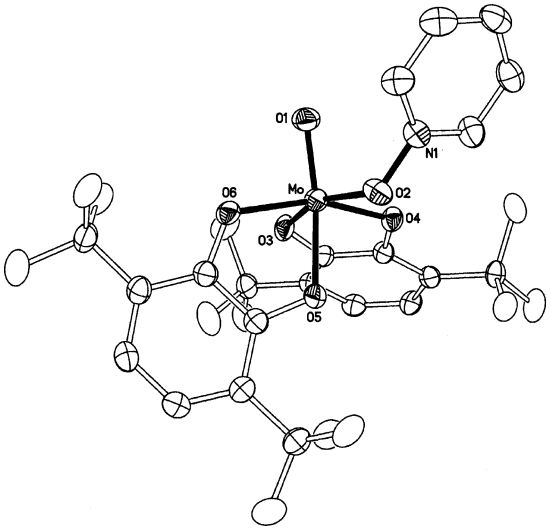

Figure 6. View showing the cis coordination of pyridine *N*-oxide in *cis*-[MoO(O-py)(3,6-DBCat)$_2$].

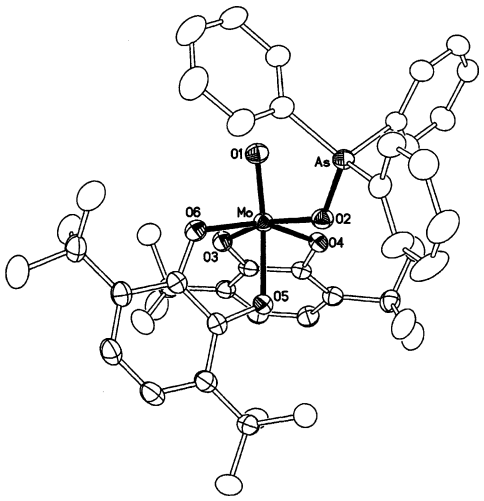

Figure 7. View showing the cis coordination of triphenylarsine oxide in *cis*-[MoO(OAsPh$_3$)(3,6-DBCat)$_2$].

formation. Slow evaporation of solvent gave crystals of [MoO(OAsPh$_3$)(3,6-DBCat)$_2$] that were suitable for crystallographic characterization. As in the case of the dmso and pyridine *N*-oxide addition products the OAsPh$_3$ ligand is found to be located cis to the oxo ligand. A view of *cis*-[MoO(OAsPh$_3$)(3,6-DBCat)$_2$] is given in Figure 7, and selected bond lengths and angles are given in Table 3 with corresponding values for the other addition products. At room temperature, the ring and *tert*-butyl proton resonances appear as broadened single resonances at 6.499 and 1.166 ppm, respectively.

Structural Features of the O-Substrate Addition Products. Metrical values for the dmso, O-py, and OAsPh$_3$ addition products are given in Table 3. It is generally found that the concentration of charge in the multiple molybdenum−oxo bond results in angles to cis ligands that are greater than 90° and typically greater than 100°. This is found to be true for the bond angles between oxo O1 in Figures 5−7 and the oxygen atoms of the catecholate ligand chelated at cis coordination sites (O3, O4). However, the oxygen (O2) of the O-Subst ligand in all three structures forms an angle close to 90° with O1. It is further surprising that in all three structures the O-Subst ligand bonds selectively at a site cis to the oxo ligand. Since monooxomolybdenum(VI) species are unusual, and there appears to be no structural characterization on addition products to five-coordinate [Mo^{VI}O(L)$_4$] complexes, there are no relevant examples for comparison. Seven-coordinate peroxo(monooxo)molybdenum(VI) complexes are common, and the peroxo group is generally coordinated at sites cis to the oxo ligand. Five-coordinate [Mo^{V}OL$_4$] species have distorted square pyramidal geometries, and addition of weakly coordinating ligands occurs at the site trans to the Mo═O bond. Examples characterized structurally include *trans*-[Mo^{V}OCl$_4$(H$_2$O)]$^-$, *trans*-[Mo^{V}OCl$_4$(CH$_3$CN)]$^-$, and *trans*-[Mo^{V}O(Cl$_4$Cat)$_2$(thf)]$^-$.[25,26] For the d^0 metals of the [MoO(O-subst)(3,6-DBCat)$_2$] series, electrostatic repulsions resulting from the strong concentration of π electron density in the Mo−O^{Oxo} and Mo−O^{Cat} bonds contribute to making the cis geometry preferred over the trans structure. Rotation of one catecholate ligand out of the tetragonal plane of the trans isomer moves the p$_\pi$-orbitals of the catecholate oxygens away from the Mo−O^{Oxo} bond. As a consequence, the O1−Mo−O6 angles in Table 3 are closer to 90° than the angles to O3 and O4. Further, the Mo d$_{xy}$ orbital of the cis isomer is in position to participate in π-bonding with catecholate oxygen O6 as a contributing electronic interaction.

Subtle features of the three complex molecules deserve comment. Structural characterization on the dmso reductase Mo center with the dmso molecule coordinated cis to the monooxomolybdenum(IV) center has shown a relatively long S−O bond length of 1.7 Å for the bound dmso.[21a] The S−O length for [MoO(dmso)(3,6-DBCat)$_2$] is more normal with a value of 1.565(2) Å.

In previous structure determinations on complexes containing quinone ligands the ligand C−O length has been viewed as diagnostic of charge, with a value of 1.34 Å considered to be normal for a catecholate ligand. In fact, values for catecholate ligands vary within the range of lengths from 1.32 to 1.37 Å.[27] This has been assumed to be random, but the pattern of C−O lengths found for the 3,6-DBCat ligands of the [MoO(O-subst)(3,6-DBCat)$_2$] series reveals a pattern. The shortest ligand C−O length in all three structures (Table 3) appears for the oxygen (O5) trans to the oxo ligand, and the longest ligand C−O lengths are found for the oxygens (O3, O4) of the catecholate chelated in the plane cis to the oxo ligand. It is of interest that the shortest ligand C−O length is found for the most weakly coordinated ligand. This is contrary to the view that strong π donation by catecholate oxygens leads to short C−O bond lengths, and weak donation leads to lengthened C−O bonds.[28] In the

(25) (a) Garner, C. D.; Hill, L. H.; Mabbs, F. E.; McFadden, D. L.; McPhail, A. T. *J. Chem. Soc., Dalton Trans*. **1977**, 1202. (b) Weller, F.; Muller, U.; Weiher, U.; Dehnicke, K. *Z. Anorg. Allg. Chem*. **1980**, *460*, 191.
(26) Manuscript in preparation.
(27) (a) Chaudhuri, P.; Verani, C. N.; Bill, E.; Bothe, E.; Weyhermüller, T.; Wieghardt, K. *J. Am. Chem. Soc.* **2001**, *123*, 2213. (b) Carugo, O.; Castellani, C. B.; Djinovic, K.; Rizzi, M. *J. Chem. Soc., Dalton Trans.* **1992**, 837.
(28) Pattison, D. I.; Levina, A.; Davies, M. J.; Lay, P. A. *Inorg. Chem.* **2001**, *40*, 214.

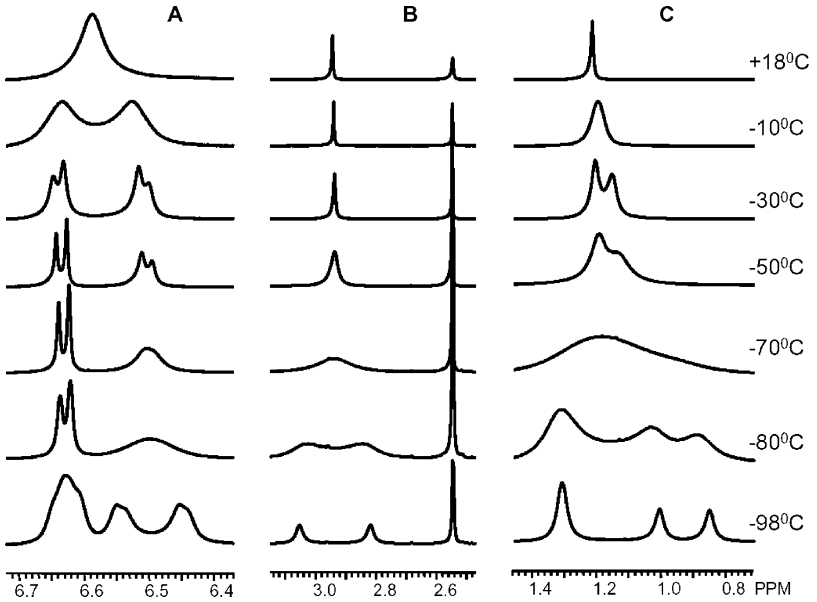

Figure 8. Temperature dependence of the ^{1}H NMR spectrum of *cis*-[MoO(dmso)(3,6-DBCat)$_2$]·DMSO recorded in CD_2Cl_2 solution.

present case it appears that the short C−O length is a consequence of the weak σ bond.

Stereodynamic Property of [MoO(dmso)(3,6-DBCat)$_2$]. ^{1}H NMR spectra recorded on all three O-Subst addition products at room temperature gave single resonances for both the ring and *tert*-butyl protons of the 3,6-DBCat ligands. This might be interpreted as indicating a trans orientation for the O-Subst ligands, but the crystallographic results clearly indicate otherwise. Spectra recorded over the temperature range between +18 °C and −98 °C for [MoO(dmso)(3,6-DBCat)$_2$] at 500 MHz, shown in Figure 8, reveal that the apparent equivalence of catecholate ring and *tert*-butyl protons is the result of dynamic site exchange. The spectrum at −98 °C consists of four resonances for the ring protons at 6.44, 6.54, and two, slightly overlapped resonances, at 6.62, and 6.64 ppm. All four ring proton resonances are split by coupling of approximately 7.5 Hz. *tert*-Butyl proton resonances appear at −98 °C as two well-separated peaks at 0.85 and 1.02 ppm, and two overlapped resonances at 1.32 ppm. Proton resonances for the dmso ligand appear as a single peak at 18 °C (2.94 ppm), but split to give two resonances (2.82, 3.05 ppm) at −98 °C.

The spectrum obtained at −98 °C is consistent with the geometry of [MoO(dmso)(3,6-DBCat)$_2$] obtained from the solid state structure. Overlapped resonances arise from a similarity in magnetic environment, and, from the geometry of the molecule shown in Figure 5, this likely occurs for the regions of the catecholate ligands associated with the trans catecholate oxygens O4 and O6. As the temperature of the solution is increased from −98 °C, peak coalescence takes place. Restricted rotation results in broadened *tert*-butyl resonances, but the pattern of coalescence remains clear for peaks of the ring protons. The two well-separated resonances at 6.44 and 6.54 ppm merge to give one half of a classic AB pattern at −30 °C; the other half of the pattern is associated with merged resonances of the protons that were slightly overlapped at −98 °C (Figure 8). The AB coupling pattern at −30 °C has been confirmed with the aid of a COSY spectrum and with spectrum simulation. At 18 °C the two components of the AB spectrum are observed to have coalesced to give a single resonance at 6.56 ppm. The four resonances observed for the *tert*-butyl protons have coalesced to give two peaks at −30 °C at 1.13 and 1.20 ppm, but at 18 °C these resonances appear as a single peak at 1.17 ppm. The dmso resonances coalesce to give a single peak at the temperature (−30 °C) where the AB pattern appears for the ring protons. Spectra were recorded on the sample of [MoO(dmso)(3,6-DBCat)$_2$] isolated as the dmso solvate used for crystallographic characterization. Consequently, a sharp dmso resonance for free dmso in solution was observed unchanged throughout the temperature range (Figure 8).

The dynamic process that averages proton resonances is nondissociative since there is no indication of dmso exchange with the free solvent. Further, changes in the three spectral regions (ring, *tert*-butyl, dmso) occur around the position of the coalesced resonance at 18 °C. This points to a simple exchange process that interchanges environmental regions of the [MoO(dmso)(3,6-DBCat)$_2$] molecule with a rate that increases with increasing temperature. The intermediacy of a trans isomer for oxo and dmso ligands would result in a completely different chemical shift for equivalent ring and *tert*-butyl protons, and an intermediate structure of this type can be eliminated. The AB spectrum of the intermediate eliminates the intermediacy of a trigonal prismatic structure with catecholate ligands chelated along trigonal faces, as the product of a Ray−Dutt twist. The appearance of an AB spectrum for the ring protons at −30 °C points uniquely to the trigonal prismatic intermediate **(I)** that results from a trigonal (Bailar) twist.[29] Constraints on the chelated catecholate ligands retain the cis disposition of oxo and dmso ligands. In the equilibrium, catecholate oxygens are distributed equally over sites trans to the oxo and dmso ligands

(29) Rodger, A.; Johnson, B. F. G. *Inorg. Chem.* **1988**, *27*, 3062.

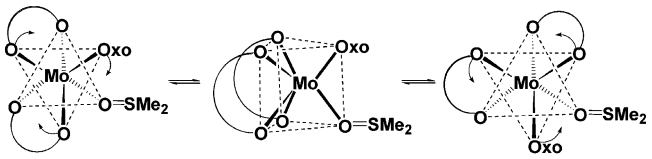

(I)

and over sites containing catecholate oxygens trans to one another. At higher temperature the rotation rate about the trigonal axis is increased, increasing the rate of racemization, and increasing the exchange rate of ring and *tert*-butyl protons among the different coordination positions.

Electrochemical Characterization on MoO(dmso)(3,6-DBCat)$_2$ and the Potential for Coordinated O-Subst Reduction. Structural features of the *cis*-[MoO(O-Subst)-(3,6-DBCat)$_2$] series place the oxygen atom of the oxidized O-Subst ligand at the site that would give a *cis*-dioxomolybdenum(VI) species upon reduction with two electrons and release of a reduced Subst species.

$$(3,6\text{-DBCat})_2\overset{O}{\overset{\|}{Mo}}\text{-O-Subst}^{Ox} + 2\,e^- \longrightarrow [(3,6\text{-DBCat})_2\overset{O}{\overset{\|}{Mo}}{=}O]^{2-} + \text{Subst}^{Red}$$

The result of a full cyclic voltammetric scan over the potential range +1.0 to −2.0 V, referenced to the Fc/Fc$^+$ potential in dichloromethane, is shown in Figure 9 for [MoO-(dmso)(3,6-DBCat)$_2$]. Two prominent redox processes appear with a number of low-current events that are associated with products of irreversible oxidation. Coupled oxidation and reduction processes appear centered at +0.455 V (vs Fc/Fc$^+$) with ΔE of 123 mV. Since the catecholate ligands are the only reduced centers of the neutral molecule, this couple is most reasonably a Cat/SQ redox process. It appears at an unusually positive potential as the result of strong π donation to the d^0 metal ion. The second prominent electrochemical feature that appears in the scan is an irreversible process at −0.852 V (vs Fc/Fc$^+$). Current measurements have shown that this is a two-electron process. The oxidized center of the neutral molecule is the Mo(VI) ion, and it is reasonable to assign this reduction as two-electron reduction of the metal. The irreversibility of the process is of interest as it may be associated with the release of dimethyl sulfide from the coordinated dmso ligand. The Mo complex that would be obtained from this process would be the *cis*-[Mo^{VI}O$_2$-(3,6-DBCat)$_2$]$^{2-}$ dianion, an ion that is well-known to form with a variety of other catecholate ligands.[22] To investigate this possibility, chemical reduction of [MoO(dmso)(3,6-DBCat)$_2$] has been carried out using cobaltocene as a reducing agent.

Reduction of [MoO(dmso)(3,6-DBCat)$_2$] with Cobaltocene. A dichloromethane solution of cobaltocene was added to a solution containing [MoO(dmso)(3,6-DBCat)$_2$] under an atmosphere of dry N_2. The color of the solution rapidly turned from the deep violet color of the dmso complex to bright orange. Catechols have been used as analytical indicators for the presence of molybdenum due to their ability to hydrolyze strongly bound oxo ligands (eq 1), and to the orange-red color of the *cis*-[MoO$_2$(Cat)$_2$]$^{2-}$ dianion that is generally obtained as a hydrolysis product.[30] This color is associated with an intense transition in the 400−410 nm region. The product of cobaltocene reduction was observed to have a strong transition at 406 nm with an extinction coefficient of 5.8×10^4 M^{-1} cm^{-1}. Crystals suitable for crystallographic characterization were obtained by slow evaporation of a dichloromethane/acetonitrile solution of the crude reduction product. The compound obtained by this procedure was found to form as a mixed CH_2Cl_2/CH_3CN solvate of (CoCp$_2$)[Mo^{V}O(3,6-DBCat)$_2$]. A view of the complex anion is shown in Figure 10; selected bond lengths and angles are listed in Table 2. The coordination geometry is square pyramidal with a clear distortion of the cis catecholate oxygens away from the apical oxo ligand to give an average O1−Mo−O^{Cat} bond angle of 110°. The reduction reaction has been followed using EPR. A signal characteristic of the [Mo^{V}O(3,6-DBCat)$_2$]$^-$ anion was observed to appear upon addition of cobaltocene to a CH_2Cl_2 solution of [MoO(dmso)(3,6-DBCat)$_2$]. It tentatively appears that one-electron reduction of [MoO(dmso)(3,6-DBCat)$_2$] leads to dissociation of dmso with formation of [Mo^{V}O(3,6-DBCat)$_2$]$^-$. Repeated scans over the potential range +1.0 V to −1.5 V led to the appearance of a reduction peak at −0.4 V that is associated with the [Mo^{V}O(3,6-DBCat)$_2$]$^-$ anion. Holm and co-workers have studied the addition of [SiCl(*t*-Bu)(Ph)$_2$] to *cis*-[Mo^{VI}O$_2$(bdt)$_2$]$^{2-}$ in a reaction that is related (in the reverse direction) to the reaction that we had hoped to observe upon reduction of [MoO(dmso)(3,6-DBCat)$_2$].[31] Electrochemical characterization on *cis*-[Mo^{VI}O(OSi(t-Bu)-Ph$_2$)(bdt)$_2$] was observed to result in formation of [Mo^{V}O-(bdt)$_2$]$^-$ in repeated scans. The decomposition reaction was attributed to proton sources in the solution, but there is similarity to the formation of [Mo^{V}O(3,6-DBCat)$_2$]$^-$ from [MoO(dmso)(3,6-DBCat)$_2$].

Conclusions

The reaction between [Mo(CO)$_6$] and 3,6-di-*tert*-butyl-1,2-benzoquinone, carried out in the presence of trace quantities of dioxygen, gives oligomers of {Mo^{VI}O(3,6-DBCat)$_2$}$_n$. It is presumed that the product formed initially is monomeric [MoO(3,6-DBCat)$_2$] with a TBP geometry similar to [MoO-{OC(CF$_3$)$_3$}$_4$]. Condensation of monomers through bridging oxo ligands gives linear oligomers with adjacent Mo centers of mixed optical stereochemistry, or the cyclic chiral [{Mo-(μ-O)(3,6-DBCat)$_2$}$_4$] square with four Mo centers of the same chirality. Condensation through the oxo ligands, together with the observed solvolysis reaction with *i*-PrOH to give *cis*-[Mo(O-*i*Pr)$_2$(3,6-DBCat)$_2$], is a consequence of a weakened Mo=O bond due to strong π donation by the catecholate oxygens. Addition of oxidized oxo-substrate ligands to [MoO(3,6-DBCat)$_2$] occurs selectively at a coordination site cis to the oxo ligand. Characterization of the stereodynamic behavior of *cis*-[MoO(dmso)(3,6-DBCat)$_2$] in

(30) (a) Page, W. J.; von Tigerstrom, M. *J. Bacteriol.* **1982**, *151*, 237. (b) Duhme, A.-K.; Hider, R. C.; Naldrett, M. J.; Pau, R. N. *J. Biol. Inorg. Chem.* **1998**, *3*, 520.
(31) Donahue, J. P.; Goldsmith, C. R.; Nadiminti, U.; Holm, R. H. *J. Am. Chem. Soc.* **1998**, *120*, 12869.

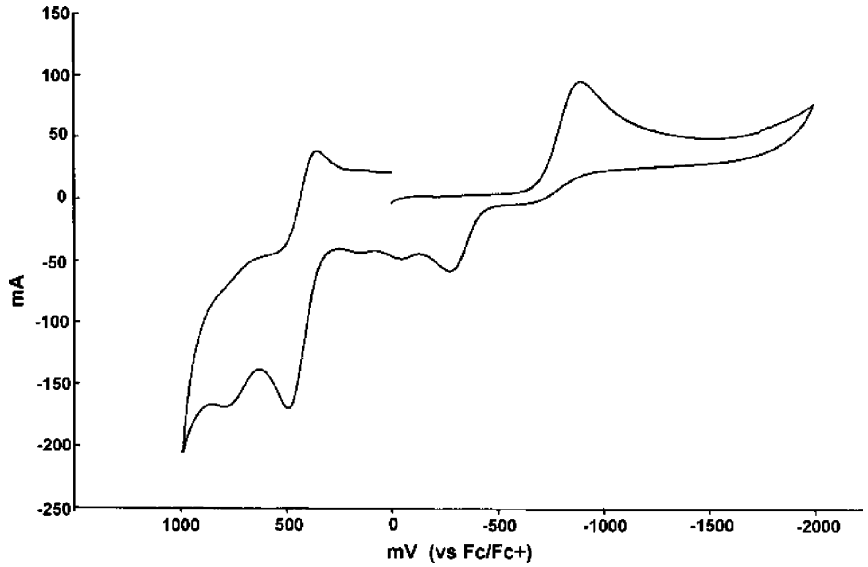

Figure 9. Cyclic voltammogram on [MoO(dmso)(3,6-DBCat)$_2$] measured in CH_2Cl_2 solution at a scan rate of 100 mV/s.

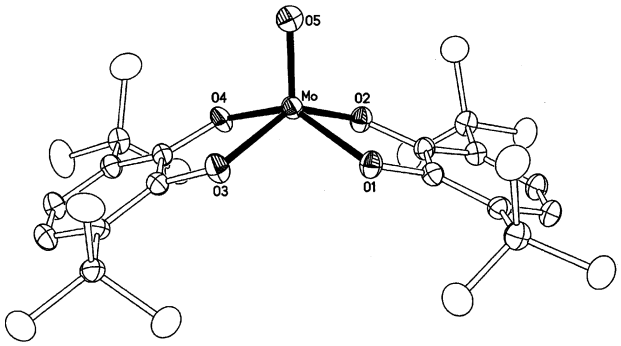

Figure 10. View of the [MoO(3,6-DBCat)$_2$]$^-$ anion obtained by one-electron reduction of [MoO(dmso)(3,6-DBCat)$_2$] with cobaltocene.

dichloromethane showed that site exchange proceeds through a trigonal prismatic intermediate, with no evidence for a structure with dmso coordinated trans to the oxo ligand. With dmso and the other O-subst ligands coordinated cis to the oxo ligand, the *cis*-[MoO(O-Subst^{Ox})] unit is poised to form a cis-Mo$^{VI}O_2$ species with displacement of Subst^{Red}. Enzymatic Mo centers release Subst^{Red} with reduction of the metal from Mo(VI) to Mo(IV). Two electrons would be required for the formation of a *cis*-[Mo$^{VI}O_2$(3,6-DBCat)$_2$]$^{2-}$ dianion from [Mo^{VI}O(O-Subst^{Ox})(3,6-DBCat)$_2$] (O-Subst = dmso, Opy, OAsPh$_3$). Experimentally, either O-Subst^{Ox} dissociation from the Mo(V) species formed upon one-electron reduction or reactivity of oxo ligands of the *cis*-dioxomolybdenum-(VI) product formed by two-electron reduction has precluded observation of Subst^{Red} displacement.

Acknowledgment. Research at Lund University was supported by the Swedish Research Council (VR). Research at the University of Colorado was supported by the National Science Foundation. C.G.P. would like to thank The Swedish Foundation for International Cooperation in Research (STINT) for a research fellowship.

Supporting Information Available: X-ray crystallographic files in CIF format for the structure determinations of the 6 compounds in Table 1. This material is available free of charge via the Internet at http://pubs.acs.org.

IC0354264